HEFAT2012
9th International Conference on Heat Transfer, Fluid Mechanics and Thermodynamics
16 – 18 July 2012
Malta

TWO-EQUATION MODEL FOR SUPERSONIC FLOWS BASED ON MODELLING OF PRESSURE–STRAIN CORRELATION

Molchanov A.M.
Department of Aerospace Heating Engineering,
Moscow Aviation Institute,
4, Volokolamskoe Shosse, Moscow
Russia,
E-mail: alexmol_2010@mail.ru

ABSTRACT

A new turbulence model K-ε-V_n for high-speed compressible flows is developed. It is based on modelling of the rapid part of pressure-strain correlation depending on Mach number and on the assumption that the velocity fluctuations normal to streamline play a key role in turbulent mixing process. Simulations of a plane supersonic mixing layers and of axisymmetrical high-speed jets are performed and comparison with the experimental data shows reasonable agreement.

INTRODUCTION

The turbulence models developed for incompressible flows fail to describe high-speed compressible flows very well. As known, compressibility in high-speed flows has a stabilizing influence on turbulence so that the intensity of turbulent mixing reduces as Mach number increases.

This effect plays an important role in present-day problems of rocket and airspace engineering. For example, in a supersonic combustion ramjet reduced turbulence levels can be highly detrimental as they reduce the rate at which fuel and oxidizer mix. Compressibility changes the nature of laminar-turbulent boundary-layer transition over hypersonic vehicles during re-entry.

According to the early works of Sarkar [1], Zeman [2], Molchanov [3,4] and others, it was assumed that compressibility effects may manifest themselves via the additional compressible dissipation. Compressible dissipation occurs at the level of small-scale turbulence.

However, the latest investigations (e.g. S.Girimaji [5]) showed that the major impact of compressibility on turbulence is implemented on large-scale levels and is associated with the fact that the action of pressure is quite different at low and high-speed regimes. Pressure-strain correlation scrambles the streamwise and stream-normal fluctuations leading to a low turbulent shear stress and decreased production.

NOMENCLATURE

a	[m/s]	Speed of sound
b	[m]	Mixing-layer Thickness
K	[m^2/s^2]	Turbulent kinetic energy
K_{ij}	[Pa/s]	Pressure–strain correlation
M	[-]	Mach number
M_r	[-]	Relative Mach Number
M_T	[-]	Turbulent Mach Number
p	[Pa]	Pressure
P	[Pa/s]	Production
u_i	[m/s]	Velocity components
V_n''	[m/s]	Velocity fluctuation normal to the streamlines
T	[K]	Temperature
x_i	[m]	Cartesian axes
y_0	[m]	Mixing-layer Centerline

Special characters

δ_{ij}	[-]	Kronecker Delta Tensor
δ_η	[-]	Spreading rate of the jet
ε	[m^2/s^3]	Dissipation rate
ε_{ij}	[m^2/s^3]	Dissipation Rate Tensor
μ_T	[Pa s]	Turbulent viscosity coefficient
ρ	[kg/m^3]	Density
σ_u	[m/s]	Deviation of Streamwise Reynolds Stress
σ_v	[m/s]	Deviation of Cross-stream Reynolds Stress

Subscripts

0	Total values of parameters
a	Nozzle exit
C	Centerline value
e	External flow, ambient

TURBULENCE MODEL

The transport equations for the transport of the Reynolds stresses $\widetilde{u_i'' u_j''}$ at high Reynolds numbers may be written as follows [6]:

$$\frac{\partial}{\partial t}\left(\overline{\rho}\widetilde{u_i'' u_j''}\right)+\frac{\partial}{\partial x_k}\left(\overline{\rho}\tilde{u}_k\widetilde{u_i'' u_i''}\right)=T_{ijk.k}+P_{ij}+\mathrm{K}_{ij}-\overline{\rho}\varepsilon_{ij}, \quad (1)$$

where:

$$T_{ijk.k}=\frac{\partial}{\partial x_k}\left(-\overline{\rho u_k'' u_i'' u_j''}+\overline{u_i''\tau_{jk}}+\overline{u_j''\tau_{ik}}-\delta_{kj}\overline{p' u_i''}-\delta_{ki}\overline{p' u_j''}\right),$$

$$P_{ij}=-\left(\overline{\rho u_i'' u_k''}\frac{\partial \tilde{u}_j}{\partial x_k}+\overline{\rho u_j'' u_k''}\frac{\partial \tilde{u}_i}{\partial x_k}\right),$$

$$\mathrm{K}_{ij}=\left(\overline{p'\frac{\partial u_i''}{\partial x_j}}+\overline{p'\frac{\partial u_j''}{\partial x_i}}\right),$$

$$\rho\varepsilon_{ij}=\left(\overline{\tau_{jk}'\frac{\partial u_i''}{\partial x_k}}+\overline{\tau_{ik}'\frac{\partial u_j''}{\partial x_k}}\right)$$

Dissipative term $\overline{\rho}\varepsilon_{ij}$, taking into account local isotropy, is modeled as

$$\varepsilon_{ij}=\frac{2}{3}\varepsilon\delta_{ij} \quad (2)$$

Pressure–strain correlation K_{ij} is expressed in terms of divergence-free tensor

$$\Pi_{ij}=\overline{p'\frac{\partial u_i''}{\partial x_j}}+\overline{p'\frac{\partial u_j''}{\partial x_i}}-\frac{2}{3}\delta_{ij}\overline{p'\frac{\partial u_k''}{\partial x_k}}$$
$$=\mathrm{K}_{ij}-\frac{2}{3}\delta_{ij}\overline{p'd''}, \quad (3)$$

which is divided into the slow $\Pi_{ij}^{(1)}$ and rapid $\Pi_{ij}^{(2)}$ parts

$$\Pi_{ij}=\Pi_{ij}^{(1)}+\Pi_{ij}^{(2)} \quad (4)$$

It is assumed that the slow part $\Pi_{ij}^{(1)}$, which has the physical sense of the tendency towards isotropy and is associated with small-scale turbulence, may be expressed by the formula, which is valid for an incompressible fluid [6]:

$$\Pi_{ij}^{(1)}=-C_1\overline{\rho}\varepsilon\left(\frac{\widetilde{u_i'' u_j''}}{K}-\frac{2}{3}\delta_{ij}\right) \quad (5)$$

where constant $C_1=1.8$ [6].

The rapid part $\Pi_{ij}^{(2)}$ is associated with large-scale turbulence. So this work is based on the supposition that the largest contribution toward the growth inhibition of mixing layers comes from it.

The results of rapid distortion theory (RDT) obtained by Girimaji et al. [5] show that the following formula can be used for $\Pi_{ij}^{(2)}$

$$\Pi_{ij}^{(2)}=C_{\Pi 1}\Pi_{ij}^{(P)}-C_{\Pi 2}P_{ij}, \quad (6)$$

and that the effect of pressure has three different regimes depending on Mach numbers:

1) In low speed flows pressure assumes the role of enforcing incompressibility and is governed by a Poisson equation. A standard incompressible pressure-strain correlation without any modification can be used (denoted as $\Pi_{ij}^{(P)}$). In this regime: $C_{\Pi 1}=1, \quad C_{\Pi 2}=0$.

2) For an intermediate Mach numbers, both inertial and pressure terms are of the same order of magnitude: $\left|\Pi_{ij}\right|\approx\left|P_{ij}\right|$. It is shown in [5] that this regime leads to a stabilization of the turbulent kinetic energy growth rate. In this regime: $C_{\Pi 1}\to 0, \quad C_{\Pi 2}\to 1$.

3) At very high Mach numbers pressure plays an entirely negligible effect compared to inertial terms such as P_{ij}. Pantano and Sarkar [7] showed that for high speeds the finite speed of sound causes a time delay in the transmission of pressure signals in the flow. Therefore in this regime we may neglect the dominant terms in the pressure-strain correlation model: $\Pi_{ij}^{(2)}\approx 0$. In this regime: $C_{\Pi 1}=0, \quad C_{\Pi 2}=0$.

The main criterion used in this work is turbulent Mach number $M_T=\sqrt{2K}/a$, and the following approximation by cubic piecewise polynomials is proposed for the functional dependencies $C_{\Pi 1}, C_{\Pi 2}$:

$$C_{\Pi 1}(M_T)=\begin{cases}1, & M_T\le\alpha_1\\ 1-3x^2+2x^3,\ x=\dfrac{M_T-\alpha_1}{\beta_1-\alpha_1}, & \alpha_1<M_T<\beta_1\\ 0, & M_T\ge\beta_1\end{cases}$$

$$C_{\Pi 2}(M_T)=\begin{cases}0, & M_T\le\alpha_2\\ C_{\Pi 2,\max}\left(3x^2+2x^3\right),\ x=\dfrac{M_T-\alpha_2}{\beta_2-\alpha_2}, & \alpha_2<M_T\le\beta_2\\ C_{\Pi 2,\max}\left(1-3x^2+2x^3\right),\ x=\dfrac{M_T-\beta_2}{\gamma_2-\beta_2}, & \beta_2<M_T<\gamma_2\\ 0, & M_T\ge\gamma_2\end{cases} \quad (7)$$

where

$\alpha_1=\alpha_2=0.1; \quad \beta_1=0.27; \quad \beta_2=0.315; \quad \gamma_2=10;$

$C_{\Pi 2,\max}=0.65$

For modeling $\Pi_{ij}^{(P)}$ the simple formula is used [6]:

$$\Pi_{ij}^{(P)} = -C_2\left(\mathrm{P}_{ij} - \frac{2}{3}\mathrm{P}\delta_{ij}\right), \tag{8}$$

where constant $C_2 = 0.6$ [6].

By taking the trace of equation (1) we obtain the transport equation for turbulent kinetic energy *K*:

$$\frac{\partial}{\partial t}(\overline{\rho}K) + \frac{\partial}{\partial x_k}(\overline{\rho}\tilde{u}_k K) = T_{k.k} + \mathrm{P}(1 - C_{\Pi 2}) + \overline{p'd''} - \overline{\rho}\varepsilon\,, \tag{9}$$

where $\mathrm{P} = \frac{1}{2}P_{ii} = \overline{\rho u_i'' u_k''}\frac{\partial \tilde{u}_i}{\partial x_k}$ - generation of turbulent kinetic energy; it is assumed that $\overline{p'd''} \approx 0$.

It is supposed that equation for turbulent dissipation rate ε has the standard form and is slightly modified from its standard form to be consistent with considering a suppressing effect of compressibility on generation:

$$\begin{aligned}&\frac{\partial}{\partial t}(\overline{\rho}\varepsilon) + \frac{\partial}{\partial x_k}(\overline{\rho}\tilde{u}_k\varepsilon) = \frac{\partial}{\partial x_k}\left[\left(\mu + \frac{\mu_T}{\sigma_\varepsilon}\right)\frac{\partial \varepsilon}{\partial x_k}\right] \\ &+ \frac{\varepsilon}{K}\left[C_{\varepsilon 1}\mathrm{P}(1 - C_{\Pi 2}) - C_{\varepsilon 2}\overline{\rho}\varepsilon\right]\end{aligned} \tag{10}$$

Thus, a closed system of equations which allow to define the Reynolds stress in high-speed flows by solving the corresponding partial differential equations is obtained.

However, it is complicated to solve this set of equations. Six Reynolds stress transport equations have to be solved simultaneously and it is a mathematical challenge. Besides there is obvious difficulty in specifying the boundary conditions of the six Reynolds stress. Based on some approximation, Reynolds stress partial differential transport equations may be simplified into algebraic expressions.

In this work algebraic stress model (ASM) is built based on the following suppositions.

It is assumed that convection and diffusion in Reynolds stress transport equations for the diagonal elements of the tensor are proportional to the corresponding terms in transport equation of the turbulent kinetic energy. In non-diagonal tensor components equations these values are set to be in balance. Hence we obtain the following algebraic equations for determining Reynolds stress:

$$i \neq j: \quad \frac{\widetilde{u_i'' u_j''}}{K} = \frac{(1 - C_{\Pi 1}C_2 - C_{\Pi 2})}{C_1}\frac{P_{ij}}{\overline{\rho}\varepsilon}, \tag{11}$$

$$\begin{aligned}&i = j: \quad \frac{\widetilde{u_i'' u_j''}}{K}\left[\frac{\mathrm{P}}{\overline{\rho}\varepsilon}(1 - C_{\Pi 2}) + C_1 - 1\right] \\ &= (1 - C_{\Pi 1}C_2 - C_{\Pi 2})\frac{P_{ij}}{\overline{\rho}\varepsilon} + \frac{2}{3}\left(\frac{\mathrm{P}}{\overline{\rho}\varepsilon}C_{\Pi 1}C_2 + C_1 - 1\right)\end{aligned} \tag{12}$$

Further simplification is obtained by using the assumption that the velocity fluctuations normal to the streamline V_n'' play the key role in the mechanism of turbulent mixing process.

Let's consider a 2D flow in which the coordinate with a subscript "1" is directed along the streamline and the index "2" denotes the coordinate normal to the streamline. Obviously, the following is true in this case:

$$\begin{aligned}&\tilde{u}_2 \ll \tilde{u}_1, \quad \frac{\partial f}{\partial x_1} \ll \frac{\partial f}{\partial x_2}, \quad f = \tilde{u}_1, \tilde{u}_2, \\ &\tilde{u}_3 = 0, \quad \frac{\partial f}{\partial x_3} = 0\end{aligned} \tag{13}$$

Then, from (1):

$$\begin{aligned}&P_{12} \approx -\overline{\rho u_2'' u_2''}\frac{\partial \tilde{u}_1}{\partial x_2}, \quad P_{22} \approx 0, \\ &P_1 \approx -2\overline{\rho u_1'' u_2''}\frac{\partial \tilde{u}_1}{\partial x_2}, \quad \mathrm{P} \approx -\overline{\rho u_1'' u_2''}\frac{\partial \tilde{u}_1}{\partial x_2}\end{aligned} \tag{14}$$

For the only non-diagonal component from (11) we find:

$$\widetilde{u_1'' u_2''} = -\frac{(1 - C_{\Pi 1}C_2 - C_{\Pi 2})}{C_1}\frac{K^2}{\varepsilon}\frac{\widetilde{u_2'' u_2''}}{K}\frac{\partial \tilde{u}_1}{\partial x_2} \tag{15}$$

Besides:

$$\begin{aligned}&\mathrm{P} \simeq -\overline{\rho}\widetilde{u_1'' u_2''}\frac{\partial \tilde{u}_1}{\partial x_2} \\ &= \overline{\rho}\frac{(1 - C_{\Pi 1}C_2 - C_{\Pi 2})}{C_1}\frac{K^2}{\varepsilon}\frac{\widetilde{u_2'' u_2''}}{K}\left(\frac{\partial \tilde{u}_1}{\partial x_2}\right)^2\end{aligned} \tag{16}$$

For $X = \widetilde{u_2'' u_2''}/K = \widetilde{V_n''^2}/K$ we obtain a quadratic equation from the equations (12) and (16):

$$\begin{aligned}&\beta(1 - C_{\Pi 2})X^2 + \left[(C_1 - 1) - \frac{2}{3}\beta C_{\Pi 1}C_2\right]X \\ &- \frac{2}{3}(C_1 - 1) = 0,\end{aligned} \tag{17}$$

$$\beta = \frac{(1 - C_{\Pi 1}C_2 - C_{\Pi 2})}{C_1}\frac{K^2}{\varepsilon^2}\left(\frac{\partial \tilde{u}_1}{\partial x_2}\right)^2 \tag{18}$$

From (15) we obtain a formula for the shear stress in the familiar form:

$$\overline{\rho}\widetilde{u_1'' u_2''} = -\mu_T\frac{\partial \tilde{u}_1}{\partial x_2}, \tag{19}$$

where the turbulent viscosity coefficient is introduced

$$\mu_T = \frac{\left(1 - C_{П1}C_2 - C_{П2}\right)}{C_1}\frac{\widetilde{V_n''^2}}{K}\overline{\rho}\frac{K^2}{\varepsilon}, \qquad (20)$$

It is assumed that the turbulent viscosity coefficient obtained via formula (20) can be applied to ALL components of Reynolds stress, and in general case the following formula is true:

$$-\overline{\rho}\widetilde{u_i''u_j''} = \mu_T\left(\frac{\partial\tilde{u}_i}{\partial x_j} + \frac{\partial\tilde{u}_j}{\partial x_i}\right) + \frac{2}{3}\delta_{ij}\mu_T\frac{\partial\tilde{u}_m}{\partial x_m} + \frac{2}{3}\delta_{ij}\overline{\rho}K, \quad (21)$$

With this approach, the equation (17) is used to calculate $X = \widetilde{V_n''^2}/K$; coefficient β, included in this equation is determined through the mean gradient of velocity

$$\beta = \frac{\left(1 - C_{П1}C_2 - C_{П2}\right)}{C_1}\frac{K^2}{\varepsilon^2}\left(\frac{\partial\tilde{u}_i}{\partial x_j}\frac{\partial\tilde{u}_i}{\partial x_j}\right) \qquad (22)$$

SIMULATION RESULTS

Testing the model involved comparing the simulation results using this model with the available experimental data for various types of flow. The computer program UNIVERSE-CFD, developed in Moscow Aviation Institute [8], was used for simulation.

Test 1. High-speed plane mixing layers

This test involved the comparison with the experimental data of Goebel, Dutton [9] and data from Ref. [5]. The experimental setup of a two-dimensional mixing layer consists of a channel with two incoming streams separated by a splitter plate. The top stream is labeled as primary and the lower as secondary. The primary stream is chosen as the high-speed inlet.

Seven mixing layer cases have been examined in [9]. For each case, static pressures were measured, schlieren photographs were taken, and flowfield velocity measurements were obtained using an LDV system. These data have been used to obtain growth rates and to examine the development of the mean and turbulent velocity fields of compressible, turbulent mixing layers. The operating conditions for the seven cases that have been examined are listed in Table 1. As is clear from this table, a wide variety of conditions have been studied with freestream velocity ratios ranging from 0.16 to 0.79, freestream density ratios ranging from 0.57 to 1.55, and relative Mach numbers ranging from 0.40 to 1.97.

Table 1

Case	1	1d	2	3
$r=U_2/U_1$	0.78	0.79	0.57	0.18
$s = \rho_2/\rho_1$	0.76	0.76	1.55	0.57
M_1, M_2	2.01, 1.38	2.02,1.39	1.91, 1.36	1.96, 0.27
T_1, T_2 [K]	163, 214	151, 198	334, 215	161, 281
U_1, U_2 [m/s]	515, 404	498, 392	700, 399	499, 92
p [Pa]	46e3	55e3	49e3	53e3

Table 1(continued)

Case	3r	4	5
$r=U_2/U_1$	0.25	0.16	0.16
$s = \rho_2/\rho_1$	0.58	0.6	1.14
M_1, M_2	2.22, 0.43	2.35, 0.3	2.27, 0.38
T_1, T_2 [K]	159, 275	171, 285	332, 292
U_1, U_2 [m/s]	561, 142	616, 100	830, 131
p [Pa]	53e3	36e3	32e3

To assess the relative performance of the new presented model (K-ε-V_n) against standard models calculations with the following three turbulence models were performed:

1. K-ε - standard two-equation model without the compressibility correction.
2. K-ε *cc* - standard two-equation model with the Sarkar [1] compressibility correction.
3. K-ε-V_n - new compressible model presented in this paper.

The supersonic mixing layer is characterized with relative Mach number:

$$M_r = \frac{U_1 - U_2}{\overline{a}} = \frac{\Delta U}{\left(a_1 + a_2\right)/2} \qquad (23)$$

Figures 1-6 compare normalized similarity profiles of Reynolds stress, cross-stream turbulence intensity and streamwise turbulence intensity with the experimental data [9] for cases 4 and 5. The mixing-layer thickness b was taken to be the distance between transverse locations where the mean streamwise velocity was $U1\text{-}0.1\Delta U$ and $U2+0.1\Delta U$. The y coordinate of the mixing-layer centerline is y_0. The standard deviations of the Reynolds stresses are defined as $\sigma_u = \sqrt{\widetilde{u_1''u''}_1}$, $\sigma_v = \sqrt{\widetilde{u_2''u_2''}}$.

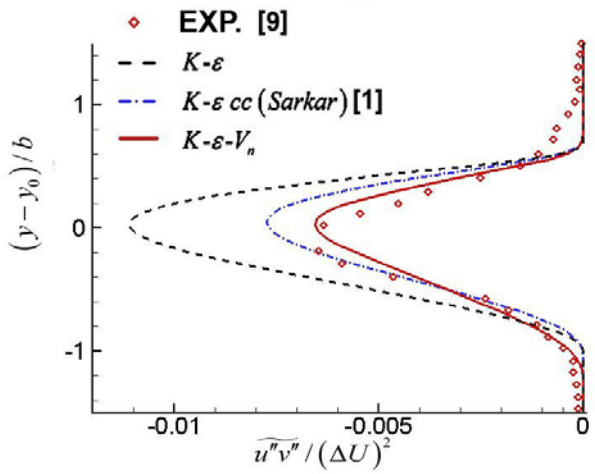

Figure 1 Similarity profiles of normalized Reynolds stress for Case 4

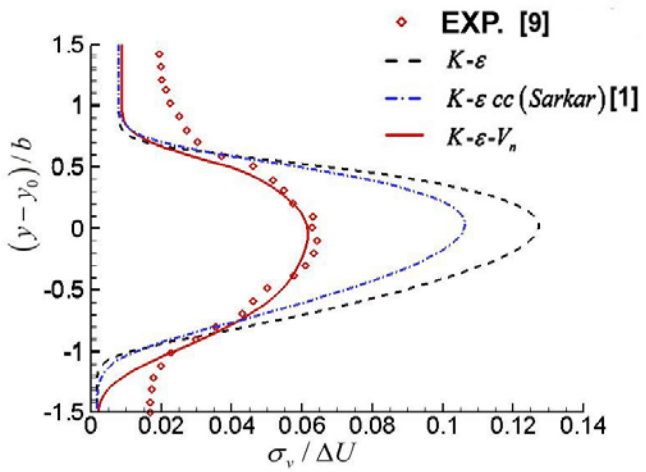

Figure 2 Similarity profiles of normalized cross-stream turbulence intensity for Case 4

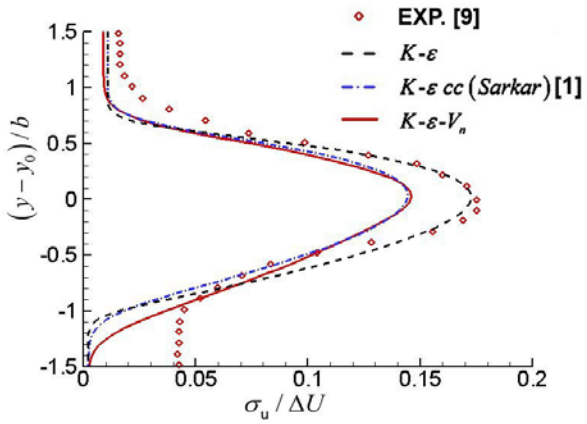

Figure 3 Similarity profiles of normalized streamwise turbulence intensity for Case 4

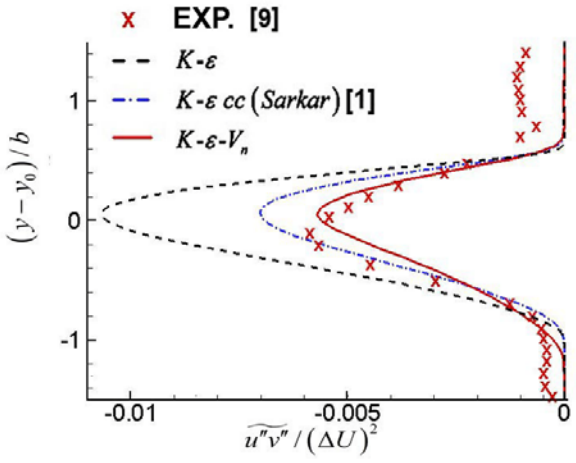

Figure 4 Similarity profiles of normalized Reynolds stress for Case 5

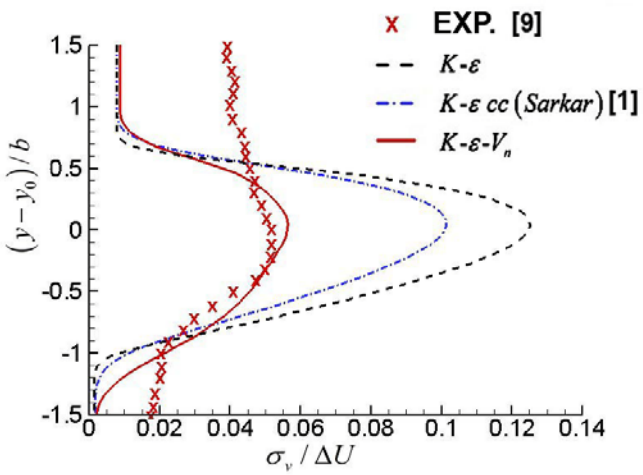

Figure 5 Similarity profiles of normalized cross-stream turbulence intensity for Case 5

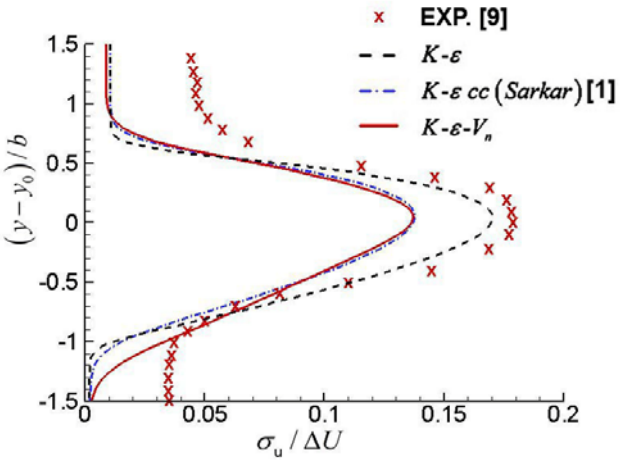

Figure 6 Similarity profiles of normalized streamwise turbulence intensity for Case 5

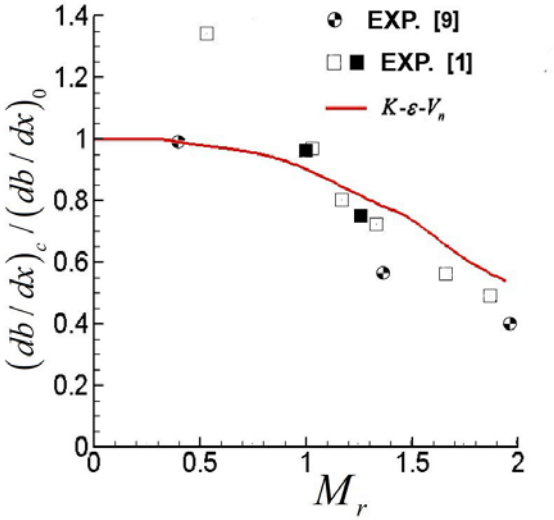

Figure 7 Normalized mixing-layer growth rates vs relative Mach number

Figures 7-10 present the mixing-layer growth rates $(db/dx)_c$ and turbulence quantities $\left(\widetilde{u''v''}/(\Delta U)^2\right)_c$, $(\sigma_v/\Delta U)_c$, $(\sigma_u/\Delta U)_c$, normalized by the corresponding quantities obtained without compressibility correction in incompressible mixing layers at the same freestream velocity and density ratios, with respect to the relative Mach number.

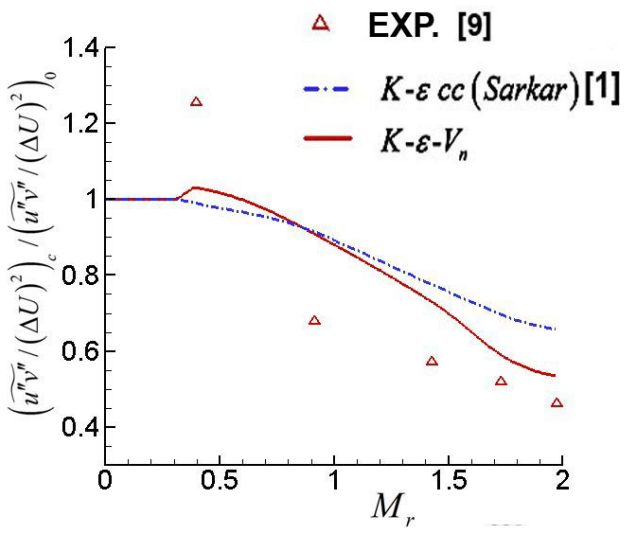

Figure 8 Normalized Reynolds shear stress vs relative Mach number

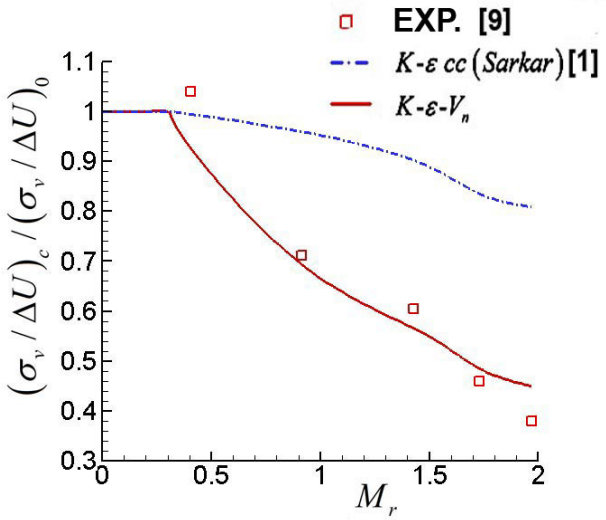

Figure 9 Normalized cross-stream turbulence intensity vs relative Mach number

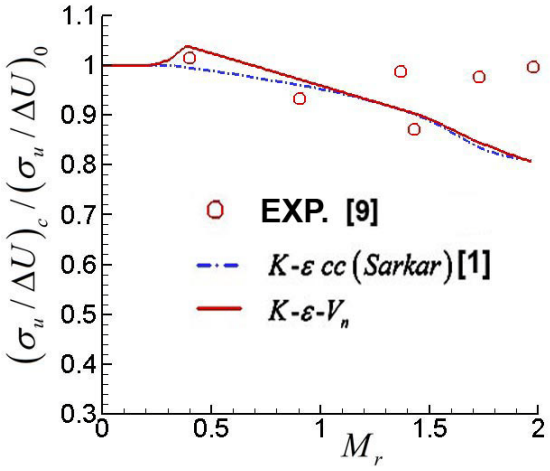

Figure 10 Normalized streamwise turbulence intensity vs relative Mach number

The results clearly show:

1) Mixing-layer growth rate reduces due to compressibility. *K-ε-*V_n yields reduced mixing-layer spreading rates at high relative Mach number, consistent with the experimental data [1,5]. Incompressible models do not capture the mixing inhibition.

2) The increase of Mach number leads to reducing shear stress (Figure 8) and to a considerable reduction of cross-stream turbulence intensity (Figure 9) as well as a very slight change of streamwise turbulence intensity (Figure 10). All these mean that compressibility, in the first place, impacts on velocity fluctuations normal to streamline, and impacts on shear stress via the value $\widetilde{V_n''^2}$ in accordance with formula (15) ; the impact on velocity fluctuations along the streamline is small. The presented model *K-ε-*V_n accounts for those facts quite well, however, the model of Sarkar et al. [1] does not.

3) The incompressible models grossly overpredict the magnitudes of shear stress cross-stream turbulence intensity.

Test 2. Fully Expanded Heated Free Jets ($p_a = p_e$, $T_a = T_e$).

This test aimed at validating the presented turbulence model for the simulation of jets, whose temperature, density and pressure at the nozzle exit are the same as those in the ambient, i.e.

$$T_a = T_e, \quad \rho_a = \rho_e, \quad p_a = p_e$$

This condition makes an estimate of a pure effect of compressibility on jet parameters. Simulations with *K-ε, K-ε cc* [1] and *K-ε-*V_n turbulence models were performed and compared.

Simulation results were compared with the experimental data of Lau et al. [10] and Krasotkin et al. [11].

Figure 11 shows the axial distribution of the mean velocity on the jet axis for different Mach numbers ($M_a = 0.28$, $M_a = 1.37$). The results exhibit a consistent trend in which the curves move downstream as the Mach number is increased. Simulations with K-ε-V_n turbulence model are in a good agreement with the experimental data and also show the increase of the jet length with the increase of M_a.

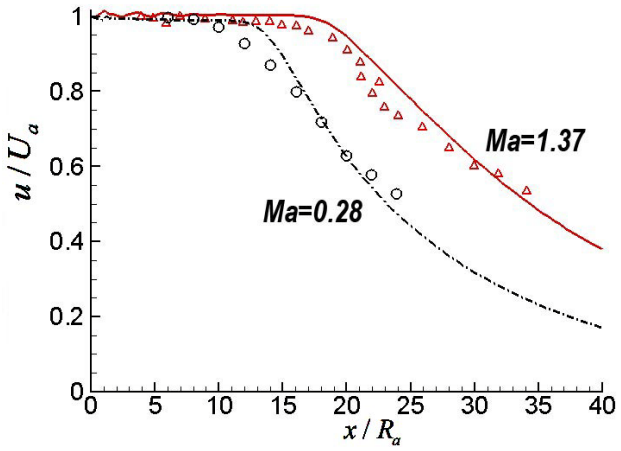

Figure 11 Normalized centerline velocity u_C / u_a vs. normalized distance from nozzle exit x / R_a. Calculation results (curves) compared to simulation data of Lau et al. [10] (symbols).

Figure 12 shows radial distributions of the axial turbulence intensity. Calculation results using K-ε cc and K-ε-V_n turbulence models are in a very good agreement with the experimental data of Lau et al. [10].

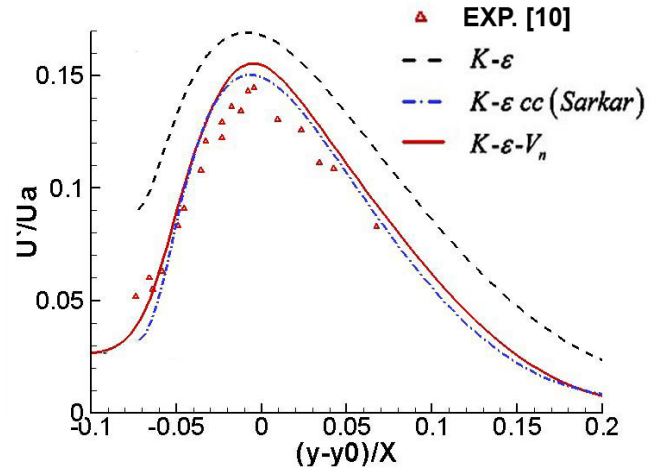

Figure 12 Radial distribution of normalized streamwise turbulence intensity for $M_a = 1.37$ at $x / R_a = 16$. Calculation results (curves) compared to simulation data of Lau et al. [10] (symbols).

It is difficult experimentally to determine the length of the isentropic zone with sufficient accuracy.

For estimation of jet length it is more convenient to use non-dimensional coordinate $\overline{X}_{0.75} = X_{0.75} / R_a$ - normalized distance from nozzle exit corresponding to the relative velocity $u_C / u_a = 0.75$ (Ref. [11]). It should be noted that in accordance with the data of Ref. [10] the maximum of the turbulent fluctuations and of the gradient of the velocity u_C is observed in the section $\overline{X}_{0.75}$.

Figure 13 shows dependence of the relative coordinate $\overline{X}_{0.75}$ on nozzle exit Mach number M_a. The simulation results (curves) were compared with the experimental data of Refs.[10,11].

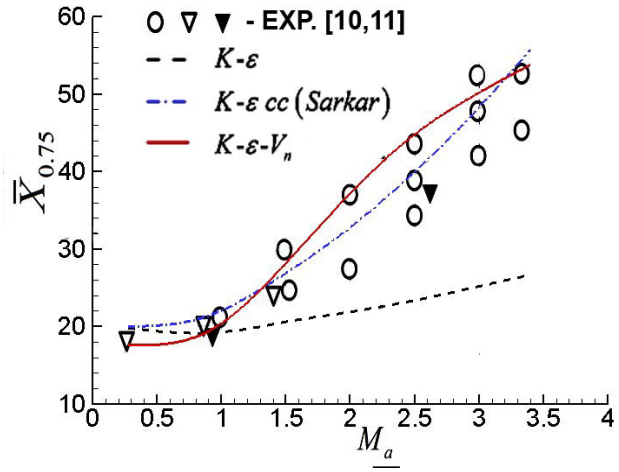

Figure 13 Relative coordinate $\overline{X}_{0.75}$ vs. nozzle exit Mach number M_a.

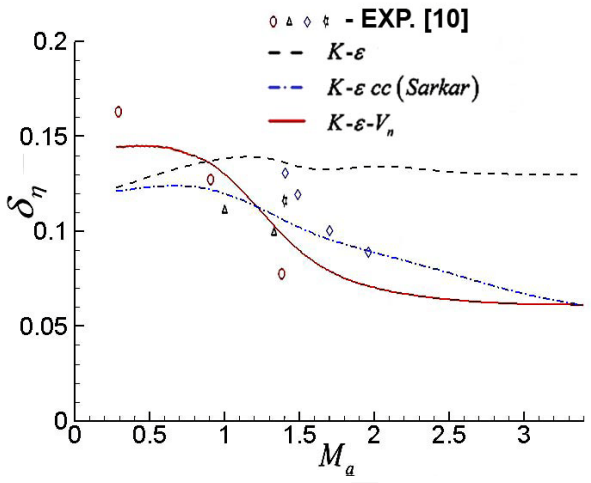

Figure 14 Relative coordinate $\overline{X}_{0.75}$ vs. nozzle exit Mach number M_a.

Figure 14 shows the variation of spreading rate of the jet δ_η with Mach number. Simulations with K-ε cc [1] and K-ε-V_n turbulence models have indicated that the spreading rate of the mixing layer decreases with increasing Mach number and are in good agreement with the experimental data.

Test 3. Cold under-expanded and over-expanded air jets at $p_a / p_e \neq 1$

This test aimed at validating the presented model for under-expanded and over-expanded air jets.

The simulation was performed for air jets having total temperature $T_0 = 300K$ and nozzle exit Mach number $M_a = 3.3$. The simulation results were compared with the experimental data of Safronov and Khotulev [12].

Figures 15, 16 present the simulation results and the experimental data for an under-expanded jet with static pressure ratio $p_a / p_e = 1.5$, diameter of the profiled nozzle $D_a = 53.7mm$ and nozzle exit half cone angle $\theta_a = 10°$.

The simulation was performed using a 400x100 trapezoidal grid. Various turbulence models were used:

1) standard K-ε model;

2) K-ε cc turbulence model with compressibility correction of Sarkar et al.[1] ;

3) K-ε-V_n turbulence model presented in this paper.

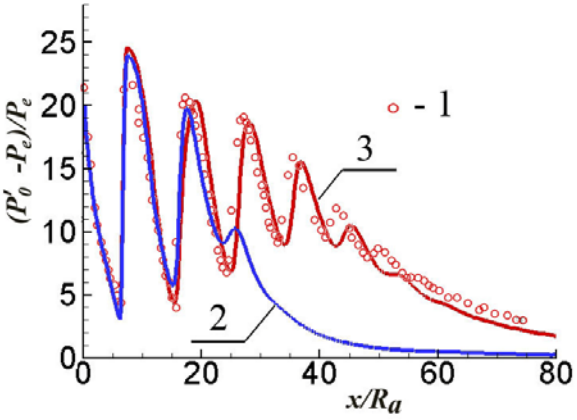

Figure 15 Centerline distribution of normalized relative pitot pressure. 1 – Safronov, Khotulev experiment [12]; 2 – simulation with standard K-ε model; 3 – simulation using present model

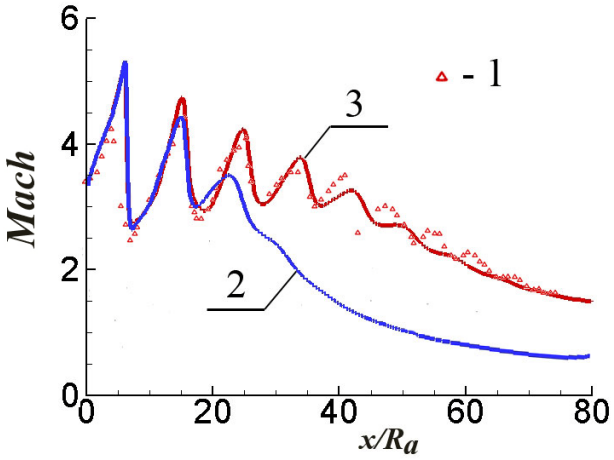

Figure 16 Centerline distribution of Mach number. 1 – Safronov, Khotulev experiment [12]; 2 – simulation with standard K-ε model; 3 – simulation using present model

Using standard K-ε turbulence model considerably under-predicts the jet length if compared with the experimental data, and also reduces a number of shock diamonds; all shock waves have significantly lower amplitude than measured.

Using the other turbulence models (2,3) gave similar results, which are in a good agreement with the experimental data of Safronov, Khotulev [12]. The pictures only illustrate the simulation results using models 1) and 3).

CONCLUSIONS

An algebraic stress model (ASM) is developed. This model is based on modeling of the rapid part of pressure-strain correlation depending on turbulent Mach number and on the assumption that the velocity fluctuations normal to streamline play a key role in turbulent mixing process.

Presented K-ε-V_n turbulence model yields reduced mixing-layer spreading rates at high Mach number, consistent with the experimental data. Incompressible models do not capture the mixing inhibition.

The turbulence quantities (Reynolds stress, cross-stream turbulence intensity and streamwise turbulence intensity) obtained from the presented model are in good agreement with data.

The turbulent model developed in this paper allows to account for the fact that compressibility, in the first place, makes a suppressive effect on velocity fluctuations normal to the streamline. It leads to the increase of turbulence anisotropy with the increase of Mach number.

The incompressible models grossly overpredict the magnitudes of Reynolds stress, cross-stream turbulence intensity, which leads to more rapid mixing in comparison with the experimental data. Besides, wave structure of supersonic overexpanded and underexpanded jets is significantly distorted: the number of barrels (diamonds) is much fewer than those in

the experiment. Too high turbulent viscosity results in too large restraining of the waves and rapid amplitude decay.

REFERENCES

[1] Sarkar S., Erlebacher G., Hussaini M.Y., Kreiss H.O., The analysis and modeling of dilatational terms in compressible turbulence, *NASA Center: Langley Research Center. Report Number: ICASE-89-79, NAS 1.26:181959, NASA-CR-181959.* 1989, 34p.

[2] Zeman O., Dilatation dissipation: the concept and application in modeling compressible mixing layer, *Phys. Fluids A.*, 1990, No.2, pp.178–188.

[3] Glebov G.A. and Molchanov A.M., Model of turbulence for supersonic reacting jets, *Investigation of Heat Transfer in Flying Vehicles (Issledovanie teploobmena v letatelnykh apparatakh), Moscow. Moscow Aviation Institute*, 1982, pp.6-11.

[4] Molchanov A.M., A calculation of supersonic non-isobaric jets with compressibility corrections in a turbulence model, *Vestnik MAI*, No.1, Vol.16, 2009, pp.38-48.

[5] Gomez C.A., Girimaji S.S., Algebraic Reynolds Stress Model (ARSM) for Compressible Shear Flows, *AIAA Paper 2011-3572*. 14p.

[6] Kollmann W. (ed.), Prediction methods for turbulent flows, *Hemisphere Pub. Corp., Washington*, 1980, 468 p.

[7] Pantano C., Sarkar S., A study of compressibility effects in the high speed turbulent shear layer using direct simulation, *Journal of Fluid Mechanics*. Vol. 451, 2002, pp.329-371.

[8] Molchanov A.M., Numerical Simulation of Supersonic Chemically Reacting Turbulent Jets, *20th AIAA Computational Fluid Dynamics Conference 27-30 June 2011, Honolulu, Hawaii, AIAA Paper 2011-3211*, 37 p.

[9] Goebel S.G., Dutton J.C. Experimental study of compressible turbulent mixing layers, *AIAA Journal*, Vol. 29. No. 4. 1991, pp. 538-546.

[10] Lau J.C., Morris P.J. and Fisher M.J., Measurements in subsonic and supersonic free jets using a laser velocimeter, *Journal of Fluid Mechanics*, Vol. 93. part 1, 1979, pp. 1-27.

[11] Krasotkin V.S., Myshanov A.I., Shalaev S.P., Shirokov N.N. and Yudelovich M.Ya., Investigation of supersonic isobaric submerged turbulent jets, *Fluid Dynamics*, Vol. 23, Number 4, 1988, pp. 529-534,.

[12] Safronov A.V., Khotulev V.A., Results of Experimental Researches of the Supersonic Cold and Hot Jet, *Physico-chemical kinetics in gas dynamics [online journal]*, Vol.6, URL: http://www.chemphys.edu.ru/media/files/2008-10-20-001.pdf, 2008.